

The International Celestial Reference System

Edward Fomalont¹

¹*National Radio Astronomy Observatory, Charlottesville, VA, USA*

Abstract. The International Celestial Reference System (ICRS) is a set of prescriptions, conventions, observational techniques and modeling required to define an celestial inertial frame. The origin of the frame is the solar-system barycenter. The ICRS was adopted by the International Astronomical Union in 1997 as the replacement of the FK5 system. The frame is called the International Celestial Reference Frame (ICRF), and is realized (defined) by the accurate position of 295 radio sources, distributed over the sky, and the accuracy of the frame orientation is about 10 microarcsec. This review will cover: the history of the development of the ICRS; the basics of the major observational technique of Very Long Baseline Interferometry; the use of the fundamental observable, the group delay; experimental strategies to optimize the accuracy; the computational methods for analyzing the large data base; the two major error limitations; and the possible of ICRS/Gaia interactions.

1. Introduction: Celestial Frames and Quasars

The Earth and all celestial objects are in motion. The astronomical determination of positions and motions, however, should be described with respect to an ‘absolute’ reference frame that is free from linear and rotational accelerations. Such a frame is called an *inertial frame* (Walter, Hans & Sovers 2000). There are two methods for determining if the frame is truly inertial: objects with no forces on them should behave kinetically (move with a constant velocity); or the non-linear motion of objects with known gravitational forces should follow the expected dynamical trajectory with no mysterious forces needed. Until the development of the ICRS, most optical reference frames were formed from both kinematical and dynamical methods. The most recent FK5 system (Frick et al. 1988) is based on the accurate trajectories of solar system objects and the position and proper motions of about 1500 well-studied stars. The accuracy of this frame is about 0.02''.

In the early 1960’s the imaging and position determination of the radio noise from the sky discovered bright discrete sources of radio emission that were associated with faint optical objects. These objects, now called quasars, were found to be smaller than 0.01'' in angular size and identified with the nuclear region of distant galaxies, often dominated by bright optical cores. Most of the objects, when identified with an optical object, had significant redshifts so their proper motion would be extremely small, and they could be considered as fixed objects in any suitable inertial frame. During this period, the technique of radio interferometry, especially very long baseline interferometry (VLBI) with antennas are separated by many thousands of kilometers, enabled the positions of quasars to be determined to $< 0.001''$ (1 mas).

Astronomers in the 1970's realized that with the properties of quasars and the advancing radio technology, a set of quasar positions could determine an inertial system that would potentially be more accurate than the FK4 (and future FK5) optically-based system. The determination of an accurate astronomical inertial frame also requires the determination of the earth rotation, precession, nutation, the location and motion of the antennas in the radio array (a measurement of crustal dynamics) and parameters describing the non-rigidity of the earth. So, geological scientists also participated in the early development and analysis of VLBI data, until earth satellite and laser ranging projects took over the surveying of the Earth in the 1980's.

In §2 after a brief introduction to radio interferometry, the determination of the main astrometric quantity, the group delay, is described, and the magnitude and nature of the major astrometric components are listed. In §3 the VLBI experimental strategies, the compilation of the data and the reduction methodologies, and the generation of the ICRF2 catalog are described. In §4 the effect of the troposphere and the finite and changing angular size of quasars, the two effects that produce the majority of the frame inaccuracy, is discussed. In §5 the future of the ICRS and ICRF and its interaction with the future space-based optical interferometers like Gaia, is summarized. Finally, the appendix contains the institutions with the staff who have labored over the last forty years to provide astronomers with the current radio inertial frame.

2. VLBI Array Fundamentals

2.1. Basic Interferometry

The response of a two-element interferometer is shown in Fig. 1. See Thompson, Moran, & Swenson (2001) for a complete reference to most aspects of radio interferometry. A radio wave from a source at a coordinate position $\hat{\sigma}$ is received at two antennas, denoted by i and j at position R^i and R^j , respectively, generally on the surface of the earth. The antenna separations are often many thousands of kilometers. The radio waves traverse through the earth ionosphere and troposphere that delay the waves by τ_{io} and τ_{tr} . The difference in the arrival time of the radio wave at each antenna is called the *geometric delay*, τ_g and is given by

$$\tau_g = \frac{1}{c} \cdot \sigma \cdot (R^i - R^j) \quad (1)$$

The radio waves are reflected from the antenna surfaces to the focal point where a feed converts the radio energy into a voltage. For the moment we will assume that the radio energy is monochromatic with a frequency, ν . The voltages generated at each antenna feed are identical in character, except for a time delay, and are transported by cable or optical fibers to a correlator where they are combined. For antennas that are more than about 100 km apart, the fluctuating voltages can be recorded on tape or on a high density storage device, and then transported physically to the location of the correlator. The signals along the two paths to the correlator experience different delays and phase changes from the antenna electronics and path-length difference, and these are denoted by τ_{in} . With these definitions, the two signals input to the correlator as a function of time, t , are:

$$V^i = A \cos(2\pi\nu t)$$

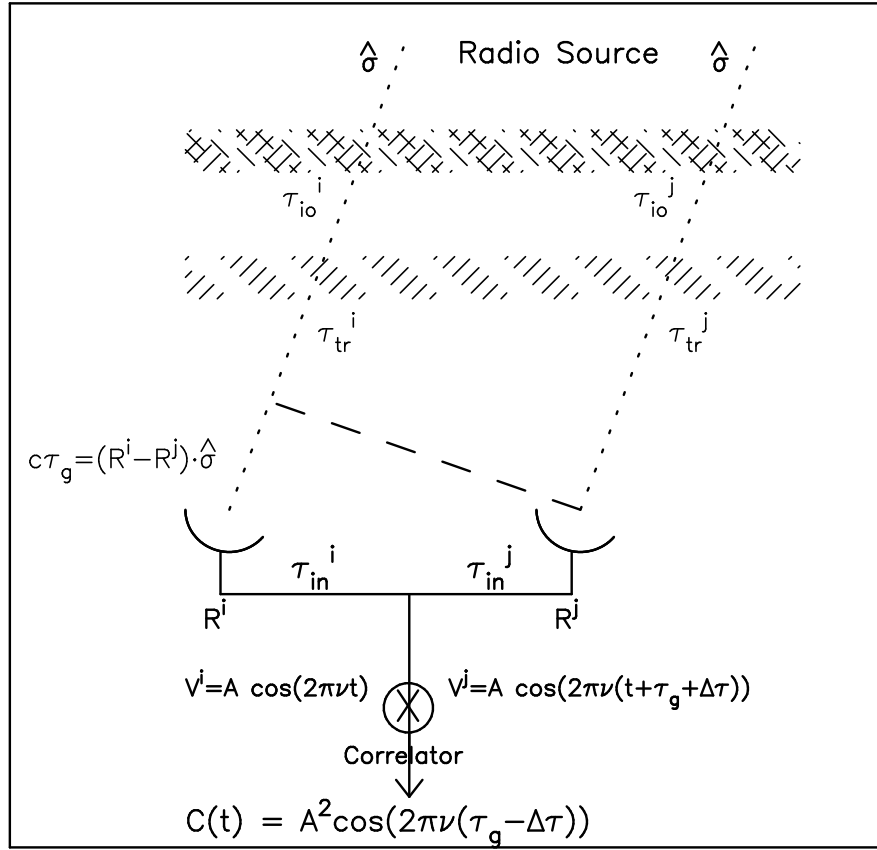


Figure 1. The Major Components of a Two-Element Interferometer

$$V^j = A \cos(2\pi\nu[t + \tau_g + \Delta\tau]) \quad (2)$$

where $\Delta\tau = \tau_{in}^i - \tau_{in}^j$. The amplitude term, A , is proportional to the intensity of the wave electric field and the gain of the antenna system.

Most correlators use digital hardware systems to multiply the two signals and integrate the product over about one second, after filtering out the high frequency ($4\pi t$) term. The correlation product $C(t)$ is

$$C(t) = A^2(t) \cos(2\pi\nu(\tau_g - \Delta\tau)) \quad (3)$$

which is simply the classical interferometric fringing between two waves of identical character as their relative phase changes. This fringe pattern has an intensity proportional to the energy in the wave with a quasi-sinusoidal variation caused by the diurnal motion of the radio source. For an observing frequency of 10 GHz and an antenna separation of 5000 km, the maximum fringe frequency caused by the earth rotation is 0.25 kHz. For an N -element array of antennas, the number of independent correlation products is the number of baseline-pairs is $N(N-1)/2$. For example, the Very Long Baseline

Array (VLBA) across the United States contains 10 antennas with 45 baselines with a maximum of 8000 km.

In order to reduce the frequency of the fringe pattern so that it can be integrated over seconds of time, a delay model, τ_M , is calculated in the correlator and the modified response becomes

$$C(t) = A^2(t)\cos(2\pi\nu([\tau_g - \tau_M] - \Delta\tau)) \quad (4)$$

This residual delay will be denoted as $\tau_r = \tau_g - \tau_M$. The components of the model delay are discussed below, but it is the best estimate of the correlator response which is dominated by the geometric delay. However, known antenna delays and estimated tropospheric antenna delay models are often included in the correlator model.

If the delay model were perfectly known, the correlator output would be a constant signal that depended on A and the residual phase between the data streams of antenna. In order to separate the amplitude and phase response, a second correlation, called the imaginary correlation, C_{im} , (the normal one is called the real correlation) is obtained by introducing a 90° phase shift between the two signals before correlation. The sum of $C + iC_{im}$ ($i = \sqrt{-1}$) is called the complex correlation. This is the normal output of most correlators and it called the observed visibility function, \mathcal{V} . It is often separated into the observed visibility amplitude and visibility phase components

$$\begin{aligned} \text{amp}(\mathcal{V}) &\equiv A_o^2 = G_i(t)G_j(t)S(t) \\ \text{phase}(\mathcal{V}) &\equiv \phi_o = 2\pi\nu([\tau_g - \tau_M] - \Delta\tau) \end{aligned} \quad (5)$$

where the visibility amplitude is composed of the gain (amplification of each antenna system times the intensity of the source, S).

Even with accurately determine delay models, the phase contribution from $2\pi\nu(\tau_g - \tau_M)$ is often many turns of phase, so the relationship between the observed phase the the residual geometric delay is ambiguous. This is usually the situation for arrays longer than about 200 km for which delay models cannot be determined more accurately than about 3 mm, the delay that will produce one turn of phase at 10 GHz observing frequency. A phase-related observable, called the group delay, alleviates this phase ambiguity problem.

2.2. The VLBI Observable: Group Delay

All arrays observe over a relatively large frequency bandwidth in order to increase the signal strength from the celestial source or to detect emission associated with chemical species that emit in narrow frequency ranges. The response of a two-element interferometer over a wide frequency range is simply the sum from the monochromatic responses, each channel of which is,

$$C(t, \nu^j) = A^2(t, \nu^j)\cos[2\pi\nu^j(\tau_r(\nu^j) - \Delta\tau(\nu^j))] \quad (6)$$

The derivative of the phase response with frequency is called the group delay, G , and is given by

$$G(t, \nu) = 2\pi(\tau_r - \Delta\tau) + 2\pi \left[\frac{d\tau_r}{d\nu} - \frac{d\Delta\tau}{d\nu} \right] \quad (7)$$

If the frequency coverage is sufficient dense so that there are no phase turns between the closest channels, the group delay can be obtained with no ambiguity. The first term

is simply the residual (observed minus model) delay plus an instrumental delay. The second term, called the dispersive delays, are discussed in §2.4.

2.3. Obtaining Accurate Residual and Total Group Delays

The astrometric usefulness of the group delay has to overcome several disadvantages. First, the source response over each frequency channel must have sufficient signal to noise in order to determine a accurate slope. Second, the accuracy of the group delay depends linearly on the total frequency bandwidth that is used to determine the phase slope. Third, non-linearities in frequency of the group delay (the second term in Eq. 7) complicate the group delay relationship with the astrometric parameters. Each of these will be discussed in more detail later, but a summary of the three problems are:

- There is nothing profound about avoiding the first problem. Only sufficiently strong sources should be used with this type of astrometric measurement in order to obtain sufficiently accurate group delays.
- A technique called bandwidth synthesis observes a small number of channels, but with frequency gaps, so that a bandwidth is spanned that is much larger than the frequency sum of the channels (Rogers 1970).
- The non-linearity of the phase with frequency is a problem. The two major components of this non-linearity are phases changes associated with the antenna electronics and the delay caused by the ionosphere.

An example of using bandwidth synthesis to determine an accurate group delay is shown in Fig. 2. The data is a simulation of the results from one baseline for a scan (a continuous observation) of about 1 min of data for a strong source. Each point shows the average phase over the scan for each frequency channel. There are six groups of channels separated in frequency, with each group having 16 channels. The phase with frequency was assumed to be linear, and random noise was added to the simulated data. The total bandwidth in all of the channels is 1.0 GHz, but the spanned bandwidth is 4.4 GHz. Even though there are phase lobe ambiguities between each of the channel groups, there is sufficient signal-to-noise to connect all of the phases with a straight line.

The group delay value and error estimate for this example is $G = 830 \pm 7 \times 10^{-12}$ sec. If this data were taken with a 5000 km baseline that is typical of a VLBI separation, the delay between the two antennas is $D = 16.7 \times 10^{-3}$ sec. The astrometric sensitivity can be approximated by the angular displace of the source in the sky needed to change the geometric delay by the approximate group delay error: $\Delta G/D$. This corresponds to an angular scale of 4.1×10^{-9} rad or 0.26 mas. This is impressive angular resolution. A typical experiment consists of many antennas (the VLBA has ten antennas and 45 baselines) and about 200 scans in a 24-hour period, so that nearly 10,000 group delays are measured. This implies that the ultimate angular sensitivity of such an experiment would be much less than 0.26 mas; however, the non-random change of some delay contaminants and the large number of parameters that must be determined limit the precision of most VLBI experiments.

The total delay is the basic observable for any baseline/scan. It is the sum of the residual delay determined from the data plus the model delay that was used during the correlation of the data. The total delay obtained for each scan is used as the fundamental input to the analysis software.

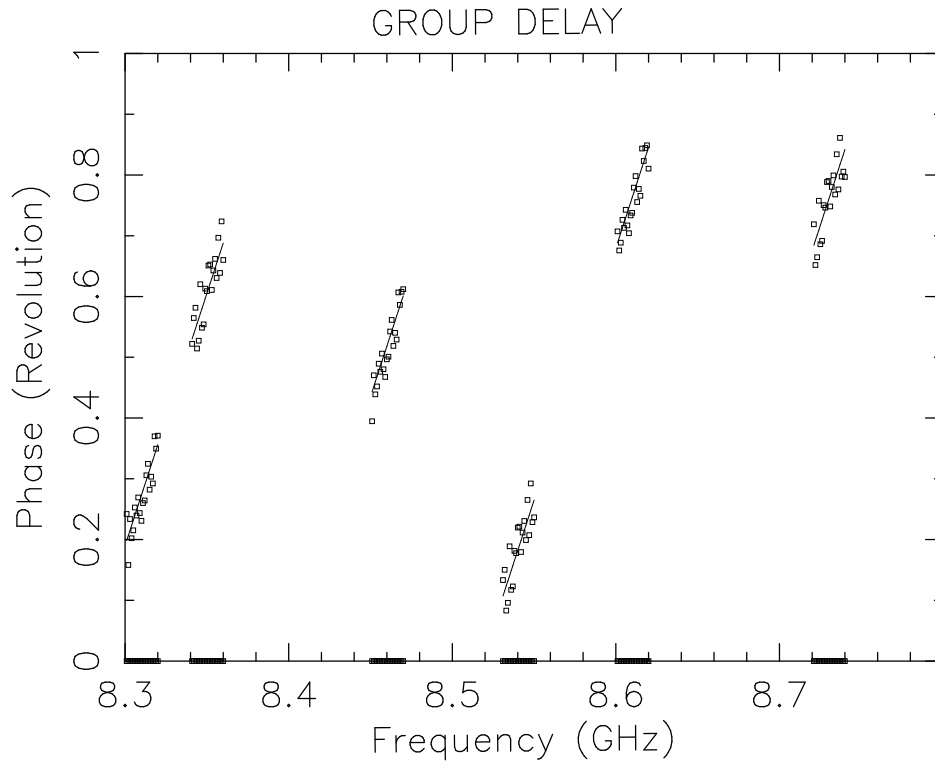


Figure 2. An Example of Measuring the Group Delay

2.4. Dispersive Delay Components

There are two major delay components that are dispersive. First, antenna systems have components that produce phase changes, rather than delay differences. For example, the six groups of channels shown in Fig. 2 often have relative phase offsets among them. Until these offsets are removed, a linear fit over the entire frequency span is not possible. Phase offsets such as these are generally constant over periods of hours and days and can often be measured using internal monitoring signals or test signals.

The other significant dispersive delay is produced by the ionized media of the ionosphere or the solar corona. The ionosphere delay is significant at the most common astrometric VLBA frequency of 8 GHz, and is variable from year to year (especially the solar 11 year sunspot cycle) and from night to day. A typical delay at 8 GHz is about 100 mm or about 300 psec which is a factor of 50 larger than the estimate delay uncertainty obtained from a scan on a strong source from one baseline. This delay varies as ν^{-2} and can be removed by observing a radio source simultaneously at two significantly different frequencies. The removal of the ionosphere delay was so critical to accurate astrometric results, that all antenna systems developed after 1975 that were used to provide astrometric support were outfitted with dual-frequency systems, with the choice of S-band = 2.3 GHz and X-band 8.6 GHz.

Table 1. Delay Components and Uncertainties in VLBI Experiments

| Component | Model Delay (mm) | Res Delay (mm) | Comments |
|------------------------|---------------------|-------------------|-------------------------|
| Geometric Delay: | 4×10^9 | 13 | All components |
| Source Position | 20 | 1 | Grav. Bending |
| Antenna Separation | 30 | 5 | |
| Antenna structure | 1000 | 4 | Deformations |
| Earth orbital motion | 6×10^5 | 1 | |
| UT and polar motion | 2×10^4 | 2 | |
| Nutation/Precession | 3×10^5 | 5 | |
| Tectonic motion | 100 | 1 | |
| Tidal motion | 500 | 3 | |
| Nontidal motion | 50 | 5 | |
| Instrumentation(clock) | 30000 | 5 | Maser signal/clock |
| Ionosphere (8 GHz) | 100 | 10 | Removed using two freq. |
| Troposphere | 2000 | 20 | |
| Source Structure | 50 | 10 | Small but variable |

2.5. Comparison of Delay Components

The major delay components that are associated with most earth-based VLBI astrometric experiments are shown in Table 1. The first column gives the component associated with the delay between two antennas. The second column in the approximate size of the model delay, the third column is the typical residual delay from which the astrometric, geodetic and other parameters can be obtained. Comments are given in the last column. A more complete discussion of these delay components are given in Sovers, Fanslow & Jacobs (1998).

The first group of components is associated with the geometric delay, and has been split into their various parts. For this table, a 5000 km separation between antennas and an observing frequency of 8 GHz is assumed. The total geometric delay is comparable to the antenna separation, and the typical residual delay after removing the best model is about 13 mm. At this frequency $1\text{mm} = 3\text{ psec}$ (3×10^{-12}). The model and typical residuals for the individual components of the geometric delay are also given.

The last four components deal with delay/phase errors not associated with the geometric delay. The largest of these come from the independent frequency standard (often called the clock) at each antenna. A pure sine wave signal is generated (usually by a Hydrogen maser oscillator) and is combined with the radio signal induced voltage in order to convert it to a lower frequency for ease of transport and processing. Time tags are also added to the data stream from accurate clocks at each antenna. The time differences among the antenna clocks are large, often 100 nsec or more, but are stable and can be easily measured from the group delay.

The ionospheric delay can be removed with dual frequency observations as described above. However, the tropospheric residual delay is large, variable and direction dependent and difficult to model or to measure. It is discussed in more detail in §4.1. The last component is associated with the non-pointlike and variable nature of the quasars and is discussed in §4.2.

3. VLBI Astrometric Procedures

The residual delay is produced by many contributions, and each of these components produces a different angular and temporal dependence that depends on the orientation and length of separation of the baseline. Since there are many parameters to determine besides the angular position of the radio source—the earth orientation and rotation properties; the antenna behavior electronically and structurally; the changing media above each antenna; the motion of the earth’s crust (antenna velocity) and cyclical tidal motions—observations of many compact sources covering the sky and with observations over a large part of the sidereal day are needed. This provides the data from which the robust solution of hundreds of parameters can be obtained. First, the observing sequence and philosophies are given, and then the several analysis stages are outlined. Finally the determination of the ICRF2, the current set of 295 sources with accurate radio positions that define the celestial inertial frame are outlined. See Ma et al. (1998) for more details.

3.1. Observing Procedures and Other Technologies

The properties of most VLBI astrometric/geodetic observations use the following observing strategy:

Number of antennas: At least five antennas are generally used, covering separations from 300 km to 8000 km. The longer the baseline the more accurate results, although accuracy beyond 5000 km baselines does not increase much because many observations must be made at low elevations. For specialized observations for determining the daily changes of earth rotation rate, observations of a few long baselines over an hour are sufficient.

Scan Length: A scan is one observation of a source using all of the antennas in the array. The main criteria for its length are : 1) sufficient duration so that the group delay determined for each baseline over the scan is sufficiently accurate which mean at least five times the signal to noise; 2) a duration not longer than the coherence time limited by the troposphere and ionosphere refraction that produce temporal phase non-linearities, and 3) sufficiently short scans so that several hundred can be made over a 24-hour period. For all these reasons, a scan length of about 30-sec to 3-min is typical.

24-Hour Observing Sessions: Many of the unknown parameters produce a characteristic delay change that has a sidereal period, but with arbitrary amplitude and phase. Hence, the algorithmic separation and maximum orthogonality in determining the parameters are improved with a 24-hour observations.

Rapid, complete sky coverage: In order to measure the changing properties of the troposphere and ionosphere, a sequence of source scans that covers a large part of the sky in 30-min to 60-min are needed to estimate the residual zenith path delay and other large-scale asymmetries.

Simultaneous dual frequency observations: As discussed above, the most accurate method to remove the ionospheric delay is to observe simultaneously at two frequencies. Thus, most arrays and antennas used for precision astrometry can observe at 2.2 GHz and 8.3 GHz simultaneously.

Wide-spanned bandwidths: The group delay accuracy varies directly as the bandwidth that is spanned in each scan. At 2.2 GHz, a spanned bandwidth is about 0.1 GHz; at 8.3 GHz, it is about 0.45 GHz.

Reporting of Results: The earth rotation and orientation from the many short and frequent observations and the longer large array observations are given by the International Earth Rotation Service (IERS) and can be found at <http://www.iers.org/IERS/EN/DataProducts/data.html>

Before 1980, VLBI observations provided much of the data about plate tectonics, through the position and motion of the radio antenna, and one of the early NASA/GSFC astrometric projects was called the 'Crustal Dynamics Project'. Since then other technologies have provided more accurate geodetic parameters than that from VLBI techniques. These groups are: Global Positioning System (GPS), a space based navigational system; Lunar Laser Ranging (LLR), earth-moon distance monitoring; Satellite Laser Ranging (SLR), Ground ranging from many earth-orbiting satellites; Doppler Orbitography and Radiopositioning Integrated by Satellite (DORIS), Doppler shift of earth beacons impinging satellites.

For the data compiled by these other technologies, a corresponding terrestrial system of rules has been developed. It is called the International Terrestrial Reference System (ITRS) and one of its goals is to determine a set of fiducial positions that defines the International Terrestrial Reference Frame (ITRF). These sites determine a frame that has no translations and rotation over time at the level of less than 1 mm/year. See <http://itrf.ensg.ign.fr/>.

These technologies have provided the VLBI analysis with extremely accurate geodetic information that have replaced that obtained previously by VLBI alone. Hence, the VLBI observations now concentrate on two aspects that cannot be done with near earth satellites: Determining the earth orientation in space, the media above each antenna, and the position of quasars and the celestial reference frame.

3.2. The Data Compilation and Reduction Methodology

The data base used to determine the ICRF2 catalog, as well as the other astrometric and geodetic parameters, includes 4540 observations sessions, most of them 24 hours long, between Aug 1979 and March 2009. These sessions cover 13 years of data over 30 years of time. There are many arrays and combinations of independent antennas that were used (see Fig. 3), so that most antennas were involved with such experiments once every two weeks or one month. The VLBA produces the most accurate results, and it has been used every two months with other several antennas in order to obtain the most accurate radio structures and longer term nutation and earth rotation parameters.

The total number of group delays obtained (from each scan \times baseline \times frequency) is 6.5 million. Over this period about 3500 radio sources were observed, although a few hundred were observed often and many have become the fiducial points for the quasar reference frame. This data archive was organized by the NASA/GSFC group.

The data reduction consists two major parts. The first is called Calc and it gathers the data for one 24-hour session with the myriad of needed bookkeeping. The software then determines the best model delay associated with each scan, using the most up-to-date parameters from previous VLBI campaigns and other technologies. This Calc model delay is more accurate than the model used in the array correlators so that a new residual delay, equal to the total observed delay minus the Calc model is the main

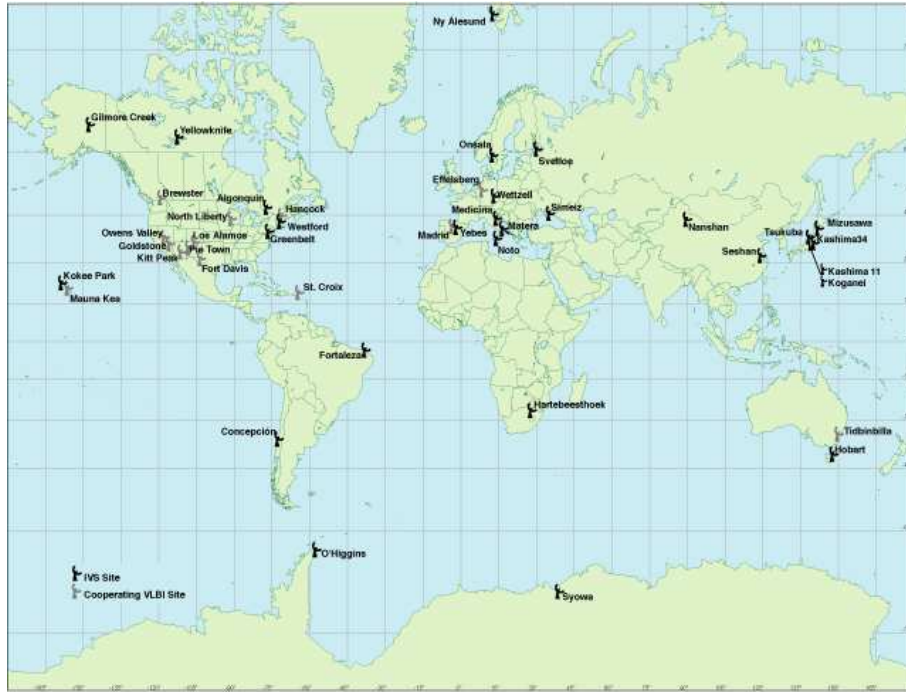


Figure 3. The International VLBI Service Network

processing parameter. The partial derivatives of the delay with respect to the unknown parameters are calculated by Calc in order to set up the non-linear least-squares solution method.

The second part of the data reduction consists of the quasi-linear least-squares solution to determine the unknown parameters associated with the 24 hour session. There are four major systems in use: Calc/Solve (Ma et al. 1998), SteelBreeze (Biermann 1977), OCCAM (Titov et al. 2004) and QUASAR (Kurbudov 2007). The parameter solutions for each sessions, and the combination of many 24-hours sessions are described in the next section. The most uncertain parameter set are associated with the tropospheric delay over each antenna.

3.3. Session Solutions and the Troposphere

For each session, about one hundred parameters are determined from the set of group delays. The parameters that are treated as constant over the day are: the antenna position on the ground (3 parameters), The UT1 rate and zero point, the polar motion (X, Y), and the two nutation terms. Some of the quasar positions may be considered fixed or the position, but others can be determined from a session (Petrov et al. 2006).

Parameters that vary during a day are the clock delay and the tropospheric delay. The clock delay between antennas is temporal, regardless of the radio source observed, and is fit using a spline or a moving average with a typical time-scale of about 30 min that includes about 15 scans. A typical clock delay is 50 nsec with a smooth variation of about 0.02 nsec per minute.

The troposphere delay over each antenna is a function of both time and angular position of the source, and its uncertainty is the largest error contribution to an astrometric experiment. The time-scale and angular scale of the changes cover seconds to seasons, one degree to the entire sky. An estimate of the global tropospheric delay can be determined from the ground weather conditions and this is included in the Calc model. Correction to this model are obtained by the observations of sources over the sky in a period of 30 to 60 min. The residual group delays are fit to a spherically symmetric model with an elevation dependence that is related to the assumed height of the wet component (1km) and dry-component (5km). In order to introduce asymmetry in the model, an e/w and n/s gradient are now added to the tropospheric delay model, each with a time scale of about 3 to 6 hours. GPS signals can be used to determine the troposphere delay in directions to the satellite.

The short-term residual delay changes over time scale of seconds to minutes are produced by small-scale dry air and water vapor refraction. These fluctuations vary between 0.1 cm for a dry high location to 10 cm during humid and stormy weather. Methods for alleviating the short-term fluctuations are discussed in §4.1.

3.4. Global Solutions, the ICRF1 and the ICRF2

After the individual parameters are derived from each session, the remaining long-term or constant parameters are determined from a global solution of all data. The most important parameters are the antenna positions and velocities with antenna deformation terms, and the radio source positions that are assumed fixed in the sky. Long term changes in nutation and tidal effects are also adjusted to obtain the best fit to the data. Adjustments of the antenna positions are made in order to be consistent with the zero point and orientation of related sites in the ITRF. Similarly, a translation and orientation of the set of radio source positions can be adjusted to be consistent with an existing reference frame, as discussed below.

In 1995 when the volume and accuracy of the radio observations exceeded that of previous optical data, the ICRF1 list of 212 sources were chosen to define an improved inertial system. The typical position error for a radio source was about 0.3 mas and the orientation accuracy of the frame was 0.03 mas. It was defined to be as continuous as possible with the FK4 optical frame.

In 2009 with the addition of 15 years of more accurate data, the radio positions of over 3500 radio sources were obtained. The improved inertial frame was based on the position of the most stable and brightest 295 radio sources, and nearly 1500 of the sources that were observed at least two times were also tied to this inertial frame. Using the positions of the 138 common sources that were in the ICRF1 and ICRF2 defining sources, continuity of the inertial frame between the two sets of sources is accurate to 0.03 mas. The position accuracy for a good quality ICRF2 radio source is about 0.06 mas and the improved inertial frame has an accuracy of 0.01 mas. The sky distribution for the ICRF2 defining sources is given in Fig. 4.

A detailed description of the ICRF2 and the other astrometric and geodetic products that are obtained can be obtained from <http://www.iers.org>. See note 35.

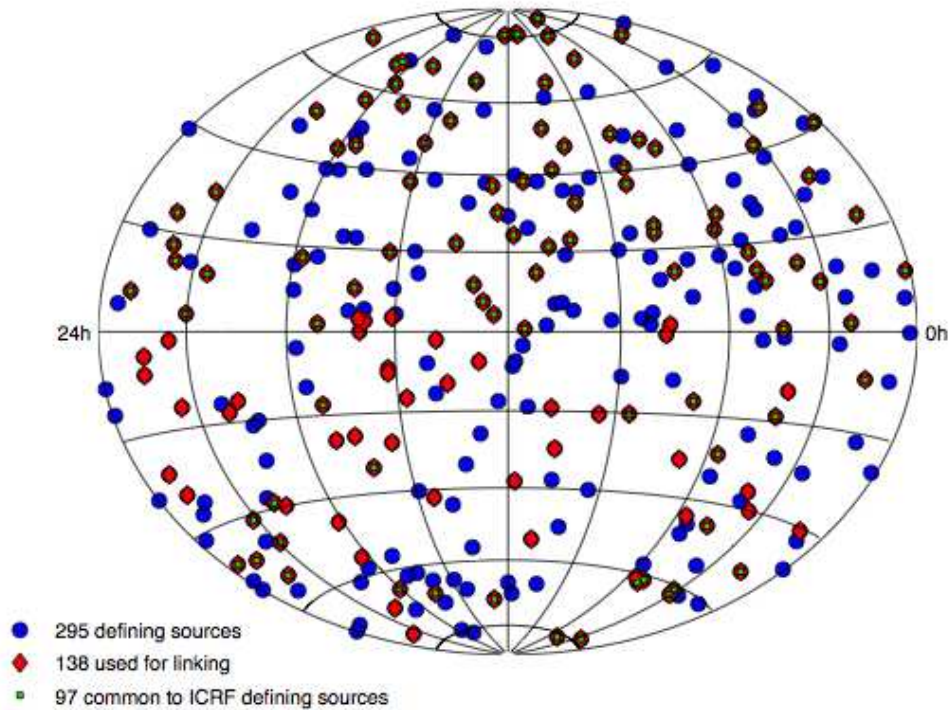


Figure 4. The Sky Distribution for the 295 sources that define the ICRF2

4. Improving the Inertial Frame Accuracy

4.1. Tropospheric Refraction

The positional accuracy of the ICRF2 is limited mainly by residual troposphere refraction. The troposphere produces short-term errors (from minutes to hours) that cannot be fit using the present observational techniques and analysis. In good weather for baselines of 5000 km, the typical rms residual delay error per scan after all parameter fitting is 20 psec (6 mm) and this corresponds to an approximate position error at 8.3 GHz of about 0.25 mas. With hundreds of observations in each session and many sessions, the position error for a source should average down to less than 0.02 mas if the differences between sessions were random; but they are not.

Experimental methods to reduce the effect of tropospheric refraction are being investigated. Faster slewing around the sky would permit refraction models with finer angular scale and a new project called VLBI-2010 is designed to use small antennas that can move more quickly over the sky (<http://www.fs.wetzell.de/veranstaltungen/vlbi/tecspec2012/>). The use of GPS satellite telemetry to measure the tropospheric delay in several directions from an antenna has an accuracy of 1 cm which is helpful in the modeling of the troposphere from the data. The use of water vapor radiometers attached to each antenna that measure the atmospheric water vapor emission in the direction of the radio source is being used successfully with the Atacama Large Millimeter Array (ALMA) in Chile (<http://www.mrao.cam.ac.uk/projects/alma/fp6/wvr.html>). However,

dry-air refractivity is still be a problem and is not measured with water vapor radiometers.

A more important astrometric error is that caused by long-term systematic effects that are associated with the models that are used to determine the tropospheric refraction. Over the last decade two improvements in modeling have been made. First, a north-south gradient has been added to the spherically symmetric model that is fit to the group delays. This gradient is caused by an average systematic north-south temperature gradient from the equator to each pole at any antenna site. Any east-west gradient related to weather fronts will tend to average out over time. The success of the additional n/s gradient term is shown by the better agreement in the declination of sources near the equator that are measured with northern hemisphere versus the position from southern hemisphere arrays at the level of 0.3 mas.

Placing an array in space would eliminate the tropospheric and ionosphere delay problem entirely, but space astrometry will probably be limited to optical arrays in the near future.

4.2. Quasar Variability

An example of the effect of structure changes on the apparent position of a quasar is shown in Fig. 5. The source 0554+242 is nearly unresolved with the ICRF2 observations and is one of the defining 295 radio sources. Because of the relatively low resolution of the ICRF2 frequency of 8 GHz, the emission of this source appears nearly unresolved (large-scale contours) although the 43 GHz image (small-scale contours) shows the the emission is composed of two components. Based on five observations over 2010 at 8, 15, 23, and 43 GHz, the radio core has been identified with the compact component to the lower right (location '0', and it is the stationary point of the source, near the galactic nucleus. The component to the upper left is extended and has been moving away from the core over the last five years. Since the peak intensity of the moving component is bright, the center of emission that is measured at 8 GHz in 2010 (location 'B') has been moving away from the core. The ICRF2 position (location 'A') based on many observations is consistent with the location of this moving component about five years ago, and is about 0.5 mas from the radio core. The structure changes for three additional sources are given in Fomalont et al. (2011).

Many apparently compact sources at 8 GHz have similar substructure that can only be followed at higher frequency (higher resolution) over a period of a year in order to determine the location of the radio core that is fixed in the sky. It is estimated that the change of position of most quasars changes by an average of 0.2 mas over months to years. Since the celestial inertial frame is defined by 295 quasars, the net affect on the frame is at the indicated error of about 0.01 mas. However, the position stability of any particular sources can be as large as 0.5 mas over a decade.

Recent observations to establish a reference frame at 23 and 32 GHz, where the effects of structure changes are less severe (because the radio core tends to be more dominant at higher frequencies), have nearly reached the astrometric precision of the ICRF2 with much more limited observations (Jacobs & Sovers 2008; Charlot et al. 2010; Lanyi et al. 2010). However, with decades of observations at 2.3 and 8.6 GHz, the radio inertial frame will likely remain attached to these lower frequency observations.

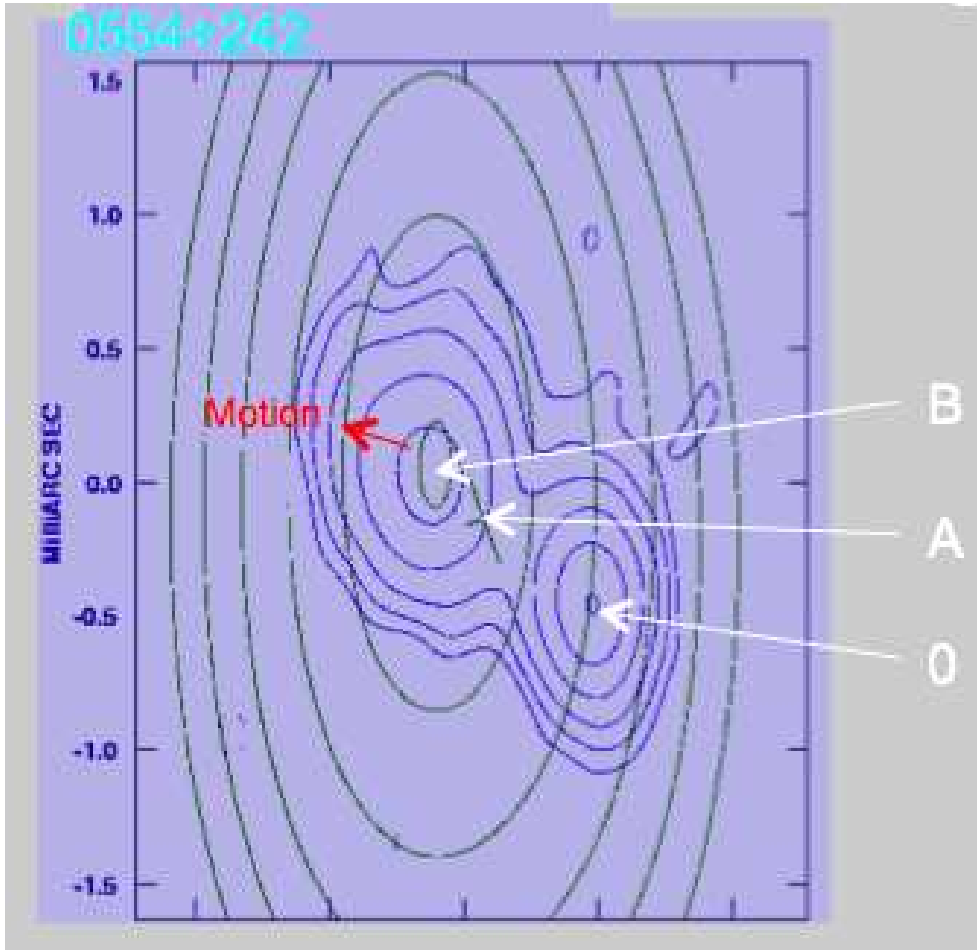


Figure 5. The Structure of Quasar 0554+242: A=position in 8 GHz ICRF2 catalog; B=position at 8 GHz in 2010, shown by the large-scale contours; C=position of radio core based on the 43 GHz contours. The component to the upper left is moving away from the core at 0.2 mas per years.

5. The Future Inertial Frame

The radio reference frame, as defined by the ICRS, will slowly increase in accuracy over the next 10 years because of better tropospheric modeling and assisted measurements and monitoring the structure changes in quasars. The VLBA2010 mission also offers the determination of a more accurate ICRF.

Many optical arrays in space have been proposed over the last decade, and one of them, Gaia, will be launched by the European Space Agency in 2013 (http://www.esa.int/export/esaSC/120377_index_0_m.html). The spacecraft at the L2 Lagrangian point will scan the sky in two directions simultaneously and build up the accurate position of more than a billion stellar objects over about a 5 year lifetime. The astrometric accuracy will be about 0.024 mas for objects brighter than about 15-mag, decreasing to about 0.15 mas for objects as faint as 20-mag. It is expected that after analysis of the mission data,

an inertial system based on these observations will be more accurate than that of the ICRF.

The transition from the radio reference frame to the Gaia reference frame, around 2020, will probably use quasars that are point-like at both optical and radio frequencies. The overlap between the brighter optical quasars with the brighter radio sources will be a small number, but sufficient numerous to tie the frames to the 0.01 mas level. It is probable that the center of light of any optical object will be displaced from the radio by 0.1 mas or more, but the large number of objects will provide a good calibration between the Gaia and the ICRF2 frame. The highest Gaia astrometric sensitivity of brighter stars can be compared with their radio positions even if only modest radio emitters. However, the parallax and proper motion of the stars must be determined before such comparisons can be made.

6. Partial List of Personnel Involved with the ICRS

Many institutions around the globe, and hundreds of scientist, engineers and computer scientists have spend enormous energy and time in helping to develop the radio reference frame. A partial list of these people is given below. Apologies for omitting many hundreds of others. NASA/GSFC: D Behrend, T Clarke, D Gordon, E Himwich, D

McMillan, C Ma, L Petrov, J Ryan, N Vandenberg,

USNO: D Boboltz, T Eubanks, A Fey, R Gaume, K Johnston, D McCarthy, R Ojha, N Zacharias

JPL/Caltech: M Cohen, J Fanslow, C Jacobs, G Lanyi, D Shaffer, O Sovers

MIT/Harvard/Haystack: T Herring, A Niell, A Rogers, I Shapiro, A Whitney

NRAO: B Clark, C Bare, E Fomalont, K Kellermann, J Romney, C Walker

Belgium: S Lambert

France: C Arias, A Baudry, C Barache, P Charlot, A-M Gontier, G Petit, J Souchay

Germany: S Böckmann, J Böhm, G Engelhardt, A Nothnagel, B Richter, H Schuh, V Tesmer, B Werl

Italy: G. Bianco

Russia/Ukraine: S. Boloton, A Finklestein, Y Kovalev, S Kurbudov, Z Malkin, E Skurikhina, Y Yatskiv, V Zharov

Australia: D Jauncey, R Heinkelmann, O Titov, C Phillips, J Reynolds, A Tzioumis

South America: A Andrei, H Hase

China/Japan: E Kawai, Y. Koyama, T. Kondo, H. Kuboki, G Wang, X, Zhang, Y Zhao

References

- Biermann, G. J. Factorization Methods for Discrete Sequential Estimation, Vol. 128, Mathematics in Science and Engineering Series, Academic Press, New York, 1977
- Charlot, P, Boboltz, D, Fey, A., Fomalont, E., Geldzahler, B., Gordon, D., Jacobs, C., and 5 coauthors, 2010, *Astron. J.*, 139, 1713
- Fomalont, E, Johnston K, Fey, A., Boboltz, D., Tamoaki O.& Honma, M 2011, *Astron. J.*, 141, 91
- Fricke, W., Schwan, H., Lederle, T., U. Bastian, R. Bien, G. Burkhardt, B. Du Mont, R. Herring, R. J ahrling, H. Jahrei, S. R oser, H.-M. Schwerdtfeger, H. G. Walter, 1988, Fifth

- Fundamental Catalogue (FK5), Part I: The Basic Fundamental Stars, Ver off. Astron. Rechen-Institut Heidelberg, no. 32, pp. 1106
- Jacobs, C.S. & O. J. Sovers, Extending the ICRF to Higher Radio Frequencies: Global Astrometric Results at 32/8 GHz, in International VLBI Service for Geodesy and Astrometry, Measuring the Future, Proceedings of the Fifth IVS General Meeting: A. Finkelstein and D. Behrend (eds.); pp. 284288, Nauka, Saint Petersburg, 2008. <ftp://ivscc.gsfc.nasa.gov/pub/general-meeting/2008/pdf/jacobs.pdf>
- Kurbudov, S. 2007, Global Solution and Daily SINEX, in Proceedings of the 18th European VLBI for Geodesy and Astrometry Working Meeting, ed. by Johannes Boehm, Andrea Pany, and Harald Schuh, GEOWISSENSCHAFTLICHE MITTEILUNGEN, Heft Nr. 79, pp. 7982
- Lanyi, G., Boboltz, D., Charlot, P., Fey, A., Fomalont, E., Geldzahler, B., Gordon, D, Jacobs, C. and 5 coauthors, 2010, *Astron. J.*, 139, 1695
- Rogers, A. R. R. 1970, *Radio Science*, 5, 1289
- Ma, C., Arias, E.F., Eubanks, T.M., Fey, A.L., Gontier, A.-M., Jacobs, C.S., Sovers, O.J., Archinal, B.A., Charlot, P. 1998, *Astron. J.*, 116, 516
- Petrov, L, Kovalev, Y.Y., Fomalont, E, Gordon, G. 2006, *Astron. J.*, 131, 1872
- Sovers, J., Fanselow, J. L. and Jacobs, C. S. 1998, *Reviews of Modern Physics*, 70, No. 4
- Thompson, A. R., Moran, J. M. and Swenson, G. W. Jr, "Interferometry and Synthesis in Radio Astronomy, Second Edition", John Wiley & Sons, New York, 2001
- Titov O., Tesmer, J & Bohm, 2004, OCCAM v.6.0 Software for VLBI Data Analysis, In International VLBI Service for Geodesy and Astrometry 2004 General Meeting Proc., Ottawa, Canada, editors: N. V. Vandenberg and K. D. Baver, NASA/CP-2004-212255, pp. 267-271
- Walter, Hans G. and Sovers, Ojars, "Astrometry of Fundamental Catalogs", (Springer, Heidelberg, 2000)